

# DLR'S MULTIPLE SWASHPLATE CONTROL SYSTEM: OPERATION AND PRELIMINARY TESTING

Philip Kuefmann, Rainer Bartels, Oliver Schneider  
philip.kuefmann@dlr.de, rainer.bartels@dlr.de, oliver.schneider@dlr.de  
German Aerospace Center (DLR), Institute of Flight Systems  
Lilienthalplatz 7, 38108 Braunschweig, Germany

## Abstract

This paper describes the first tests of DLR's patented, IBC-capable multiple swashplate control system. It briefly covers the preliminary activities and system modifications necessary to ensure successful testing, such as the ground vibration tests. The conducted hover tests and their respective results are discussed in detail, focusing particularly on Higher Harmonic Control and Individual Blade Control test scenarios. Numerous control modes were tested with and without blades, including 2-6/rev HHC, in-flight blade tracking, and different modes of tip path plane-splitting

## SYMBOLS

$\beta$	Blade Flapping Angle
$\Theta_C$	Lateral Primary Control Coefficient
$\Theta_S$	Longitudinal Primary Control Coefficient
$\Theta_0$	Collective Primary Control Coefficient
$\vartheta_{n,CMD}$	Commanded n/rev Pitch Signal
$\vartheta_{n,1-4}$	Measured n/rev Pitch Signal

## NOTATION

APS	Azimuth Angle Pulse Synchronizer
BVI	Blade Vortex Interaction
DLR	Deutsches Zentrum für Luft- und Raumfahrt (German Aerospace Center)
DNW	Deutsch-Niederländischer Windkanal (German Dutch Wind Tunnel)
DOF	Degrees of Freedom
GUI	Graphical User Interface
HHC	Higher Harmonic Control
HMI	Human Machine Interface
IBC	Individual Blade Control
META	Mehrfach-Taumelscheibe (multiple-swashplates)
RSG	Resistive Strain Gauge
TPP	Tip Path Plane
VAR	VollAktive Rotorsteuerung (fully active rotor control)

## 1. INTRODUCTION

Helicopters suffer from many problems mainly related to the rotor aerodynamics and the nonuniform inflow in forward flight. The most important problems are:

- high level of vibrations,
- high noise generated by the rotor,
- high power required in high speed forward flight,
- low range and limited speed of flight.

Since the middle of the last century, several theoretical studies and experimental investigations with respect to stall alleviation or speed enhancements<sup>[1-3]</sup>, reduction of vibration levels<sup>[4],[5]</sup>, noise radiation<sup>[6]</sup> and performance enhancements<sup>[7]</sup> have been conducted utilizing both active<sup>[7-12]</sup> as well as passive means<sup>[13-15]</sup>. While passive systems almost reach the limits of their capabilities, further improvements with active rotor control systems seem to be feasible as described in two surveys of the different well-known active control systems<sup>[16],[17]</sup>.

Active rotor control systems can generally be divided into two categories, depending on the location of the actuators. Systems using actuators located below the swashplate in the non-rotating frame (fuselage) are called Higher Harmonic Control (HHC) while systems with actuators in the rotating frame (rotor) are referred to as Individual Blade Control (IBC), Figure 1.

## Higher Harmonic Control Individual Blade Control

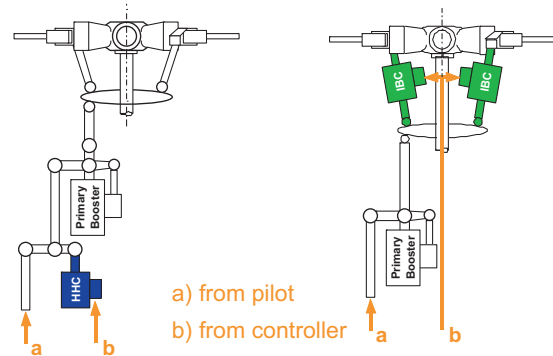


Figure 1 - Principles of HHC and IBC

Due to the significant differences in their set-up, HHC and IBC systems also differ regarding their respective advantages and disadvantages. Since HHC systems do not need electrical or hydraulic slip rings to transfer energy and signals between the non-rotating and the rotating frame, they are mechanically less complex. The HHC actuators are not subjected to centrifugal forces and a special design of the rotor hub and the blade is not necessary. Furthermore the (periodically) synchronous n/rev pitch angle variation of all rotor blades is ensured by the use of a common swashplate, which is a well proven and technically mature component. On the other hand, the greatest disadvantage of HHC is also caused by the swashplate: Due to its mechanical constraints only a limited range of control frequencies can be transmitted into the rotating frame, i.e. an integer multiple of the number of blades and the 1/rev frequency. It has been shown in various investigations that the 2/rev frequency is very useful in terms of noise and power reduction<sup>[7,10,11]</sup>. Unfortunately, this frequency cannot be controlled by HHC for rotors with four or more blades

In contrast to HHC, IBC with actuators in the rotating frame has no limitations regarding control frequencies

apart from the dynamic range of the actuators. IBC can be realized by means of several technologies whose pros, cons, and maturity level differ significantly. After the development of blade root IBC systems, a trend towards blade-integrated actuators has emerged. This includes discrete flaps (see Figure 2)<sup>[18],[19]</sup> as well as more sophisticated but less mature concepts that feature distributed piezo-microfiber actuators, integrated in the blade skin (see Figure 3) or on the blade spar, leading to a continuous blade twist<sup>[20]</sup>.

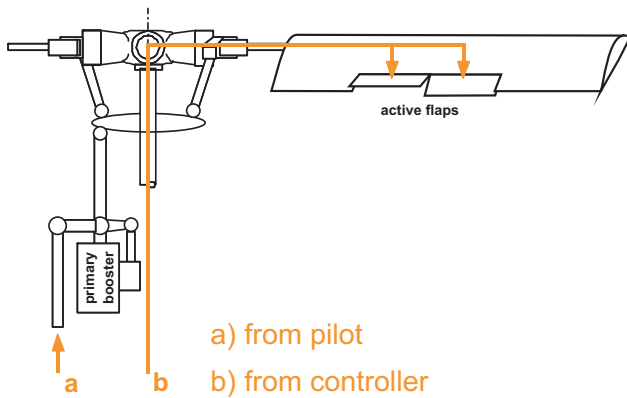


Figure 2 - Principle of Active Trailing Edge Flaps

An advantage of this concept compared to active flaps is the complete lack of mechanical parts and the homogeneity of the blade in terms of mass distribution, etc.

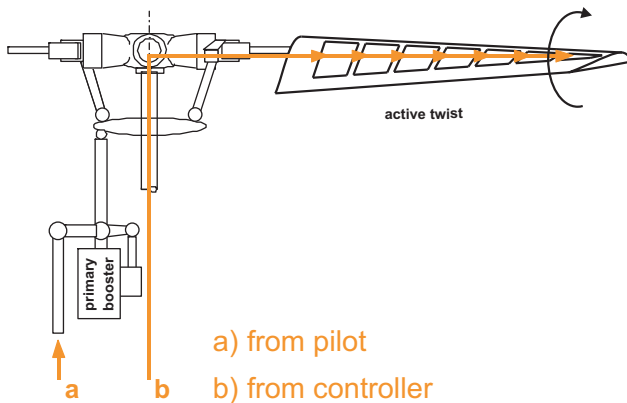


Figure 3 - Principle of Active Twist blades

While all IBC approaches offer great potential, they still share certain disadvantages. Lacking a common swashplate, the effort to ensure synchronous movement of all rotor blades is significantly higher than with HHC. Since all actuators are located in the rotating frame, an electric or even a hydraulic slip-ring is necessary adding a considerable amount of complexity and weight to the overall system. With active flaps or active twist, complexity is also a great issue in terms of rotor blade design. This is due to the already demanding task of accurately tuning the eigenfrequencies of the blade, high centrifugal loads, elastic blade deformations, influences of climatic conditions and many more reasons. Consequently it must still be proven that these systems (based on piezo-electric actuators) will be as durable as conventional rotor blades and maintenance free. Furthermore, sufficient wind tunnel test results of active-twist blades are not yet available.

## 2. THE WORKING PRINCIPLE OF THE META SYSTEM

In 2008 the DLR was issued a patent for the multiple swashplate rotor system called META (MEhrfach-TAumelscheibensteuerung)<sup>[21]</sup>, aiming to overcome the limitations of HHC and the disadvantages of IBC while retaining the advantages of both. Based on the principle of HHC, META achieves full IBC capability for helicopters with more than three rotor blades without using actuators in the rotating frame by introducing additional degrees of freedom (DOF) via multiple swashplates arranged in the same reference plane as illustrated in Figure 4. The number of swashplates needed is defined by a maximum of three blades per swashplate.

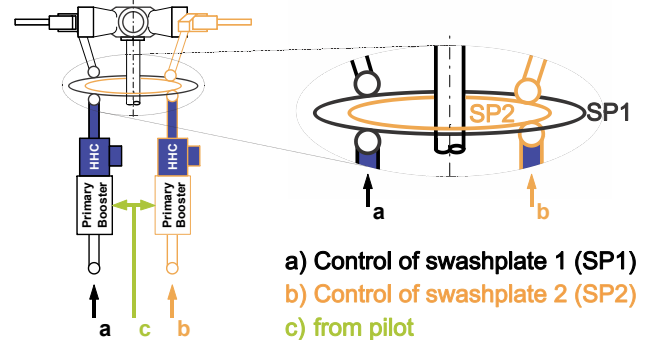


Figure 4 - Working principle of META

The META controls are superimposed onto the pilot's primary control in the non-rotating frame and directly transferred to the swashplates. Since the two (or more) swashplates are individually controlled by different sets of actuators any arbitrary position of the swashplates can be achieved. This way full IBC is obtained for every swashplate with its subset of associated blades and therefore for the whole rotor system. The META concept employs advantages known from earlier HHC projects and utilizes new control laws which have been described in<sup>[22]</sup> and<sup>[23]</sup>. The rotor hub and blades remain unchanged and the costs for maintenance of rotor components are not increased compared to conventional rotors without IBC capability. Furthermore, the swashplate itself is a well proven and technically mature system.

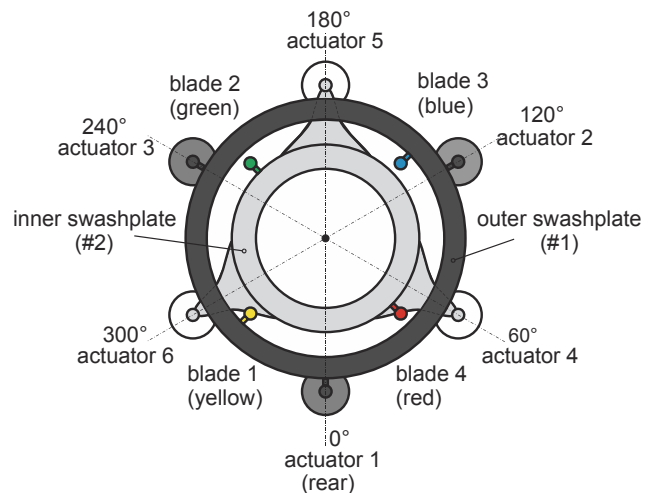


Figure 5 - Schematic of the META-system

The META system tested at the DLR facilities in Braunschweig consists of a 4-bladed 40% Mach scaled hingeless Bo105 model rotor with two separate concentric swashplates, driven by a set of six (three per swashplate) electrohydraulic actuators spaced 60° around the rotor shaft. The outer swashplate is connected to the opposing blades 1 and 3 and is driven by actuators 1, 2 and 3, while the inner swashplate is driven by actuators 4,5 and 6 and controls the blades (2 and 4). A schematic of the META-system is depicted in Figure 5.

### 3. ROTOR TEST RIG INTEGRATION

#### 3.1. Experimental Test Setup

The preliminary test was conducted in the rotor test hall of the DLR Institute of Flight Systems which is a closed wall atmospheric pressure room with a basement area of 12 m x 12 m and a height of 8 m. The META system was integrated in DLR's rotor test rig ROTEST II which was mounted on a sting support mechanism that positioned the model hub in the hall at a desired height of approx. 3 m with pitch, roll and yaw angles of 0° (see Figure 6).

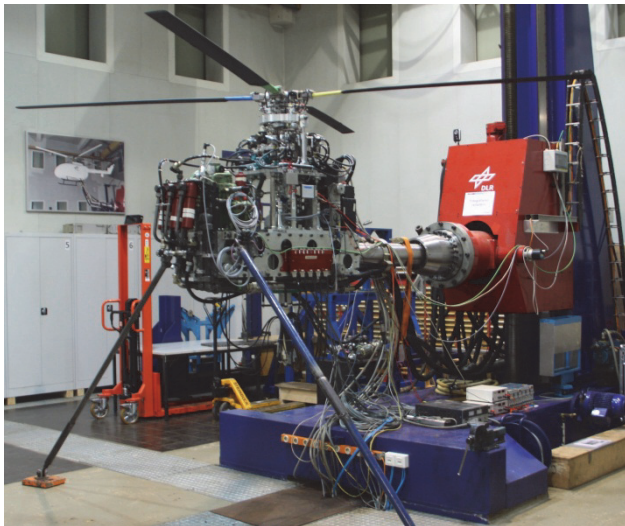


Figure 6 - META test setup at the rotor test rig

The rotor test rig is driven hydraulically with a maximum power of 130 kW and features a six component rotor balance for measurement of all rotor loads. A simplified schematic of the META-system and its components (including measurement and control hardware) is shown in Figure 7.

#### 3.2. Primary Control

The electro-hydraulic swashplate actuators (see Figure 8) consist of an electric part for the pilot's collective and cyclic control of each swashplate and a hydraulic part for controlling higher harmonic inputs. For the preliminary test the collective and cyclic control of the rotor was set by the pilot using the Human Machine Interface (HMI) to adjust both swashplates simultaneously. During the calibration phase a linear transformation matrix of actuator displacements into collective and cyclic pitch angles was determined for each swashplate and stored in the control software. Due to the slightly different and non-linear behavior of both swashplates' kinematics at different pitch settings the collective and cyclic angles of inner and

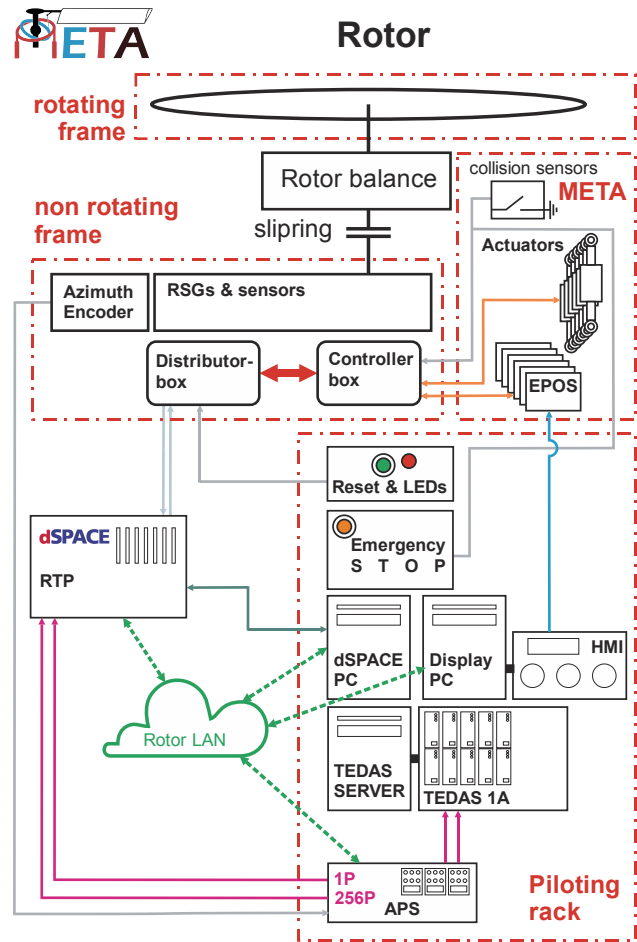


Figure 7 - Signal flow and integration schematic of the META system at the rotor test rig

outer swashplate differ up to  $\pm 0.2^\circ$ , resulting in different 1/rev control phases. Adjusting the swashplates using the hydraulic actuators would have limited the remaining control amplitudes for HHC and IBC applications and was therefore not considered for the tests. Instead, the outer swashplate was used as trim reference.

#### 3.3. HHC and IBC Control

As described in [22] and [23], the control laws to determine the actuator strokes (in the non-rotating frame) necessary to achieve the desired HHC and IBC modes were already developed in an earlier stage of the project. In the next step, a feedback controller-algorithm had to be devised to control the strokes of the hydraulic actuators (see Figure 8) within the 2/rev – 6/rev frequency range (35 – 105 Hz) with an accuracy of  $\pm 0.05$  mm in amplitude.

To accurately determine the response characteristics of the hydraulic actuators with the swashplates attached a sine sweep from 0.1 to 300 Hz was applied as input to the hydraulic control valves using a simple PID-Controller to prevent actuator runaways during the test. The measured actuator strokes as well as the sweep-signal and the output of the PID-controller were recorded as time histories. The subsequent analysis of these signals led to the identification of the response characteristics of each individual actuator which were then used for the development of the final control algorithm.

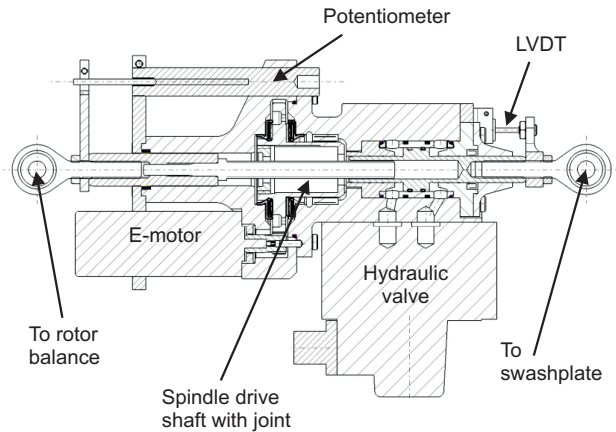


Figure 8 - Cutaway of electro-hydraulic actuator

The first control cycle consisted merely of the PID-controller used for the frequency-sweep, combined with a digital filter. This filter was added to the feedback-loop to prevent external disturbances outside the desired frequency range from affecting the control cycle. Since the PID-controller alone provided insufficient control amplitude at frequencies beyond 1/rev (17.5 Hz) and simply increasing the controller gain was not an option due to stability concerns, an “ideal” feed forward control function was designed and added to the control cycle (see Figure 9).

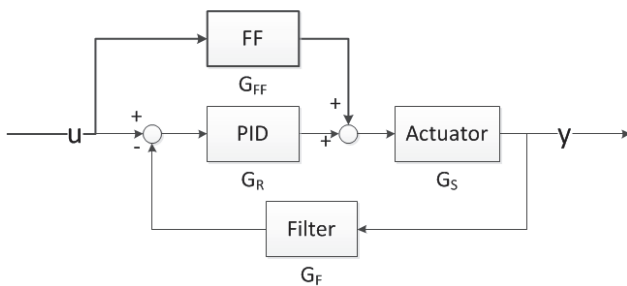


Figure 9 - Control loop including PID-Controller, Filter and Feed-Forward Control

The transfer function  $G_{FF}$  of this ideal feed-forward control is calculated from the known transfer functions of the PID-controller  $G_R$ , the actuator  $G_S$  and the filter  $G_F$  under the prerequisite of  $y = u$ , resulting in:

$$G_{FF} = \frac{1}{G_S} + G_R(G_F - 1)$$

This feed-forward control function compensates adverse effects of the filter (e.g. phase shift at higher frequencies) and uses the inverted transfer function of the hydraulic actuator to provide an additional control signal which is superimposed onto the output of the PID-controller before reaching the actuator and increases the amplitude to the desired levels. With this setup the necessary control accuracy in amplitude and phase could be achieved over the full frequency range from 0 to 105 Hz (see Figure 10).

The only remaining issue was a slight control lag, owed to the time-delay of the LVDT-sensors used to measure the stroke of the actuators. This problem was overcome simply by imposing an additional phase of  $1.5 \text{ ms} * 2\pi * f$  (approx.  $9.45^\circ$  in azimuth) onto the harmonic controller input signals. The whole controller was implemented and

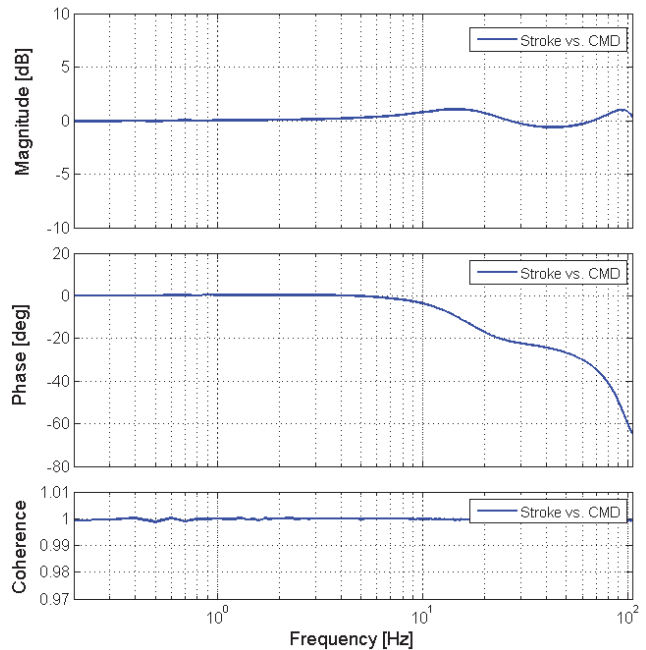


Figure 10 - Bode-diagram of closed actuator control loop (Control frequency 0 – 105 Hz)

tested in Matlab / Simulink and then compiled using the Mathworks Realtime Workshop in order to run on the dSPACE Realtime Processor<sup>[22],[23]</sup>. The dSPACE system controls and monitors all HHC and IBC functionality of the META-system and is synchronized with the rotor azimuth via two hardware interrupt signals (1/rev and 256/rev) generated by the azimuth angle pulse synchronizer (APS) from the signal of the angular encoder (see also Figure 7). With an angular frequency of approximately 17.5 Hz all control calculations are executed at frequency of 4.48 kHz in real-time.

The control software contains a graphical user interface (GUI) for controlling the HHC and IBC functions where the user can easily access and control the following modes of operation:

- Hydraulic primary control
- Single frequency HHC
- In-flight tracking (manual)
- Tip-path-plane splitting

The main panel of the piloting GUI provides access to all crucial controller functions such as emergency controller activation and reset, use of feed-forward control, determination of software limits for the actuator strokes and monitoring of rotor RPM and execution times of the different parts of the real-time program (Figure 11, left side). Furthermore, all measured actuator strokes can be monitored as min/max per revolution (right side). In another part of the GUI the actuator strokes are displayed as real-time graph every revolution and all parameters of the controller including those of the feed-forward control function can be modified on-line to account for changes of the actuators' dynamic responses for example due to changes in oil temperature or viscosity during the tests.

To ensure maximum safety during operation of the hydraulic actuators, a three-stage safety system was implemented both in software and in hardware.

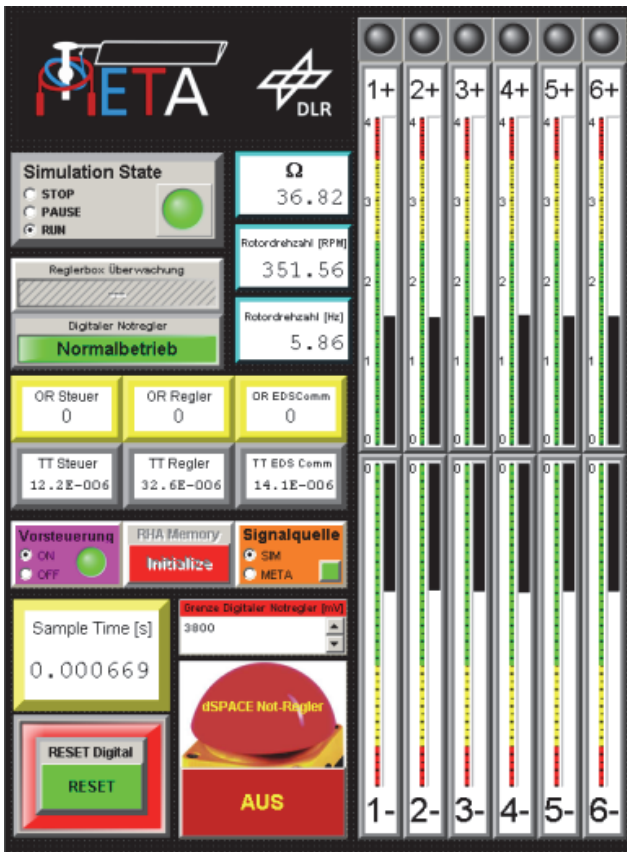


Figure 11 - Main piloting panel for actuator monitoring and position control

In case one of the measured hydraulic actuator strokes exceeds predefined software limits ( $\pm 3.8$  mm) the pre-control function is deactivated and the commanded stroke for all actuators is immediately set to 0 mm, forcing all six actuators into the neutral position regardless of current user inputs. Once all user inputs (for example HHC amplitudes) are set to zero, the controller can be reset to its normal function via a reset-button in the GUI (Figure 11, lower left corner).

Additionally, the circuit boards designed for handling the signal transfer between the dSPACE-system and the actuators incorporate a signal filter and an analogue proportional controller to take over in case the software controller or the dSPACE system as a whole should fail. This analogue “emergency controller” is activated if actuator strokes exceed limits defined and monitored via a limit comparator on the respective circuit board which are set between the aforementioned software limit and the mechanical limits of the hydraulic actuator pistons ( $\pm 4$  mm). The analogue controller can also be activated via pushbutton and by the collision sensors installed on the swashplates (see <sup>[23]</sup> and Figure 7). On activation a relay closes the analogue control loop for all six actuators, the actuators are set to neutral position and all inputs from the dSPACE-system are ignored until the system is reset manually.

### 3.4. Measurement Systems

The basic instrumentation of the test rig consists of sensors for measuring rotor rpm, rotor azimuth, blade pitch angles, torque, rotor loads, pitch link forces, and

temperatures. Furthermore there are safety of flight sensors for shaft and blade bending to monitor critical system loads. In addition to the basic instrumentation sensors for hydraulic pressure of the actuation system, actuator loads, and electrical and hydraulic actuator displacements were installed for the META project.

All signals from the rotating system are pre-amplified within the rotor head and transferred to the non-rotating system via slip-ring. The recording of the signals is done simultaneously for all channels triggered to the rotor azimuth by a data acquisition system<sup>[24]</sup> with a sampling rate of 128/rev. After trimming the model and setting of the desired control input the data acquisition is started and all raw data for 32 successive rotor revolutions are stored on disc. These data are then time averaged for each of the channels and a fast Fourier analysis up to the 16th harmonic is carried out. After preprocessing the data remain easily accessible for further analysis, visualization, or immediate printout.

## 4. PRELIMINARY ACTIVITIES AND TESTS

### 4.1. Ground Vibration Tests

For the determination of all dominant natural frequencies a ground vibration test of the model with and without blades was performed in advance. By means of a shaker system the model was excited at the rotor head in all directions with different modes (random, sinus-sweep) and force levels. By using accelerometers at six different locations the model's dynamic behavior was measured and analyzed. The first natural frequency of the total system was identified to be at 6.05 Hz. For the rotor head – balance system the eigenfrequency in longitudinal direction was found to be at 32.8 Hz and at 27 Hz for the lateral direction. For ground resonance analysis also the first lag bending frequency was identified by measuring the decay curve after release of one blade in the non-rotating system. The frequency found was 11.3 Hz. The ground resonance analysis resulted in no risk of instabilities in the rpm range used.

### 4.2. Non-Rotating Tests Without Blades

After completing the installation every subsystem of the META control system had to be tested individually. These non-rotating tests were conducted without blades as first system tests of the new control system. The main aim of these tests was to ascertain the correct realization of the control laws used for the actuators to control both swashplates of the META. Additionally, all peripheral components like electronic pre-amplifiers, secondary hardware controllers as well as all sensors, wirings and the hydraulic piping were thoroughly checked to detect possible system or control limitations for safety reasons prior to any rotational tests.

After passing all electric and hydraulic pressure tests (200 bar system pressure), the 1/rev primary control of the META was tested. The primary control is accomplished by the electric part of the actuators and is manually controlled by the test rig operator using the HMI (see 0 and Figure 7). In the primary control mode the two swashplates are placed identically in collective and cyclic position. To test the correct 1/rev placement of the swashplates simple collective ( $\pm \theta_0$ ) and cyclic ( $\pm \theta_C$  &  $\pm \theta_S$ ) inputs were used and checked manually.

During this test mode the hydraulic parts of the actuators were operated at low hydraulic pressure (<50 bar), enough to hold them controlled in their neutral position. The 1/rev and 256/rev trigger signals for the dSPACE system were simulated for full rpm (see 3.3).

After successful completion of the primary control tests using the electric part of the actuators, the hydraulic part of the actuators was tested. As described in 3.3, the strokes of the actuators are controlled by PID controllers including feed forward control. The controller parameters were set individually to match the separately identified actuator characteristics obtained from the aforementioned frequency-sweep identification. The aim of these tests was to check and adapt the individual controller parameters to best fit the commanded signals in amplitude and phase for every individual control frequency.

During these tests collective ( $\pm 3^\circ$ ) and 1/rev signals up to 2.75°, as well as single frequency signals from 2/rev (1° amplitude) to 5/rev (0.5° amplitude) were applied. Single blade tracking function of every blade was tested till  $\pm 0.3^\circ$ . Collective and 1/rev tip-path-plane splitting (TPP) was tested up to 2° difference between the two swashplates at four different control phases (0/90/180/270° → only 1/rev). 2/rev TPP was tested up to 0.5°, also at these four different phases.

Additionally, individual actuator runaways were simulated to test the collision sensors and the controller's three-stage safety system by exceeding the predefined software limits ( $\pm 3.8$  mm -  $\pm 3.95$  mm), forcing the actuators immediately towards their neutral position.

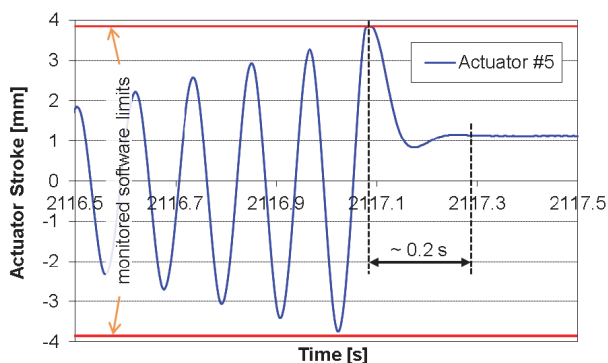


Figure 12- Dynamic test of the safety circuit

Figure 12 shows the dynamic test of the safety circuit, where the dynamic stroke amplitude of actuator 5 was linearly increased ( $\sim 4$  mm/s). When the actuator stroke reached the upper software limit the analogue emergency controller was engaged and forced the actuator to its steady stop position which is reached after about 0.2 s. Note that this position has a little offset to the neutral position due to the lack of an I-component in the analogue controller.

### 4.3. Rotating Tests Without Blades

After accomplishing the non-rotating tests, the META system was prepared for first rotating tests without blades. The main aim of these tests was to verify the correct control phases of the commanded and actual controlled actuator strokes and blade pitch angles for all frequencies tested (1/rev-5/rev). Just like the non-rotating tests before,

this started with primary control inputs (collective & 1/rev) up to  $3^\circ$  using the electric part of the actuators, while the hydraulic parts were operated at low hydraulic pressure (<50 bar) were held in neutral position.

For the subsequent primary control tests using the hydraulic part of the actuators, the blade pitch angles for 1/rev signals were tested up to  $2^\circ$ , while the collective control was tested till  $3^\circ$ .

The following single frequency tests were carried out with 360° phase sweeps (in 30° steps) applying maximum amplitudes of 1.5° at 2/rev, 1° at 3/rev and 0.5° at 4 & 5/rev. The blade tracking tasks were tested till 0.5° for single blade tracking and  $\pm 0.2^\circ$  in combination (blade 1 with 3 and blade 2 with 4).

Collective and 1/rev TPP was tested with 2° differential amplitudes of the swashplates, while 2/rev TPP was tested with a maximum difference of 1°. During 1 & 2/rev TPP a full phase sweep was applied (0/30/60/.../330°).

### 4.4. Difficulties Encountered

During the non-rotating tests some nonrelated problems occurred, leading to a necessary revision of the respective system or function. For example, applying the designed system pressure of 200 bar to the hydraulic system of the actuators lead to a clearly audible and also measurable resonance noise coming from different vibratory parts of the modified test rig. Under some operating conditions this accidentally built up to a flutter-like condition which caused mainly the outer but also the inner swashplate to vertically oscillate in their eigenfrequencies with low amplitudes ( $< \pm 0,1$  mm) resulting in very high loads ( $> \pm 4000$  N) measured in the baseplates of the actuators. The sample in Figure 13 shows one of these occasional resonances.

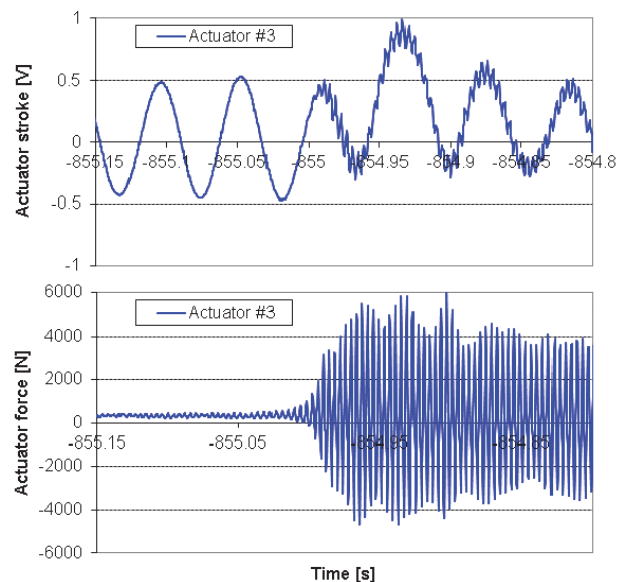


Figure 13 - Stroke and force of Actuator 3 at the onset of the resonance phenomenon

From time stamp -855 s the actuator 1/rev stroke is superimposed by high frequency disturbances with low amplitudes (note: V/mm  $\approx 1$ ), while shortly shifted in its offset. At the same time the forces measured in the baseplate below actuator 3 rise to considerable levels.

A couple of investigations showed that this phenomenon did not originate from the controller gains but mainly relates to the characteristics of the highly agile hydraulic servo valves driving the actuators with a dither-frequency of 400 Hz interacting with the eigenfrequencies of both swashplates (~250 Hz & ~400 Hz) and is increased by pressure pulsations from the hydraulic piston pump (225 Hz) and the low stiffness of the actuator baseplates.

Reducing the electronic dither amplitude of the servo valves lead to a less aggressive behavior of the actuators but also raised the inner friction of the valves resulting in poor guiding accuracy and occasional overshoots for steady inputs, so this was not a preferred solution. However, as the delivery status of the dither of all valves was dissimilar, a more evenly behavior of the actuators was obtained through equalizing the dither of all valves.

With increasing hydraulic pressure the sensitivity and the maximum forces of the actuators rose, so as a first action the maximum hydraulic pressure used for the actuators was reduced to 150 bar, limiting the actuator forces to a maximum of  $\pm 3000$  N. The reduced forces are then still high enough to hold and move the swashplates in every planned operation condition.

After reducing the pressure and equalizing the dither, the actuators emitted a softer humming noise, and the resonance did not occur again. As a side effect of this action the frequency response of the actuators changed and had to be re-identified. In addition, the feed-forward loop parameters of the controllers had to be adapted as well.

A second problem occurred before the rotational tests were started. An unstable behavior occurred while the actuators were controlled in their neutral position, building up increasing oscillatory movements up to the hardware limits. The reason for this was found in the reduced triggering frequency of the digital controller coming from the APS prior to rotating. For the rotating tests at low rpm the APS triggers the measurement, the data acquisition and the dSPACE system at a fixed simulated rotational speed (~350 rpm). When spinning up the rotor the systems get triggered from a hardware azimuthal angle encoder as soon as the real rotational speed is higher than the simulated rpm. At reduced simulated rpm the time between two trigger events is three times longer than at full rpm. Since the parameters of the digital PID controller were only designed for full rpm, the gains were too high for reduced rpm leading to unstable actuator behavior. The problem was solved implementing a linear dependency on the rotational speed, reducing the overall controller gain for lower rpm.

With these revisions the entire tests without blades showed good correlation between commanded and actual controlled signals in all frequencies, amplitudes and phases, so the next step – the main rotating tests with blades – was prepared.

## 5. TESTS AND RESULTS WITH BLADES

### 5.1. Test-Matrix and Goals

The goal of the preliminary tests was to demonstrate the functionality of the multiple swashplate system for individual blade control of a four-bladed rotor in hover conditions. The results found will be used to modify and

prepare the system for wind tunnel tests. In the planned test matrix the main control modes like primary collective and cyclic control, individual blade tracking, higher harmonic inputs from 2 to 6/rev, as well as different TPP splitting control modes were scheduled.

All tests were conducted at a rotational speed of 1041 rpm (17.35 Hz) using a nominal thrust of 2500 N. This thrust level (77% of scaled BO105 thrust) was chosen as a compromise of high thrust versus resulting turbulence level in the testing hall. The turbulences increase with higher thrust due to ground proximity and recirculation in the closed testing hall. For the 2/rev TPP splitting tests 50 % (1250 N) of the nominal thrust was used in order to keep the expected high 2/rev z-forces below the load limits of the rotor balance (see 5.5.2).

The test matrix is shown in Table 1. The numbers given are the maximum values used during the tests; the originally planned values are given in parentheses.

Table 1 - Test matrix with planned and tested values

Test case	Control frequency [n/rev]	Control amplitude [°]	Control phase [steps in°]
Collective	0	3.0 (3.0)	-
Cyclic	1	1.0 (2.0)	90 (90)
HHC	2	1.5 (2.0)	30
	3	0.75 (2.0)	
	4	0.25 (1.0)	
	5	0.3 (0.5)	
	6	0.07 (0.5)	
Tracking	0	0.5 (0.2)	each blade
TPP splitting	0	2.5 (2.0)	30
	1	0.75 (1.0)	
	2	0.5 (0.5)	

Limiting factors found during the tests were a highly dynamically loaded rotor balance, high actuator forces (up to allowed maximum), and high blade bending moments in flap and torsion.

### 5.2. Electric and Hydraulic Primary Control

The goal of the first tests conducted with the META-system was to determine rotor force and moment derivatives with respect to the primary controls. First, separate variations of collective, longitudinal and lateral control were tested with the hydraulic pistons of the actuators in neutral position ( $\pm 0$  mm) using only the electric drive. The resulting changes in forces and moments were recorded and then compared to the results of additional tests during which primary control was achieved using only the hydraulic part of the actuators. Two examples of the results are depicted in Figure 14.

Both modes of operation (electric and hydraulic) for primary control generally yielded approximately the same results in rotor balance forces and moments. The minor

differences which can be seen in Figure 14 can be attributed the slight difference in cyclic control between the two swashplates, which has already been described in 0.

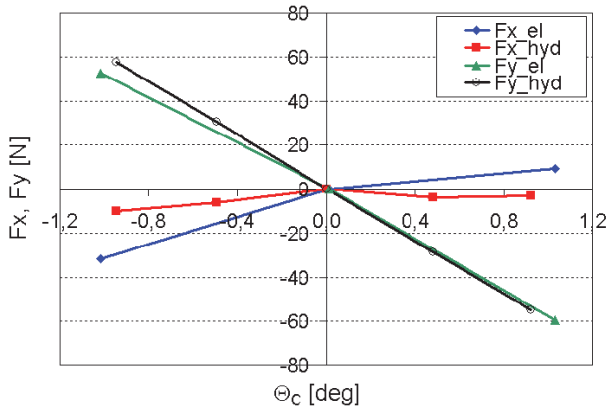


Figure 14 - Variation of longitudinal force  $F_x$  and lateral force  $F_y$  due to electric (blue) and hydraulic (red) cyclic control

### 5.3. Manual In-Flight Tracking

The manual tracking of single blades was the first “full IBC” application of the META-system. By a slight collective shift and an oscillating movement of one swashplate, the anchor point one of the corresponding pitch links (on the swashplate) was lowered independently of azimuth while the opposite pitch link stayed in its original position relative to the rotor hub. This resulted in the collective pitch angle modification – or tracking - of one single rotor blade. During the tests the pitch of the blades was successfully modified individually up to  $\pm 0.5^\circ$  and the resulting changes in hub forces measured and recorded.

After the initial tests of manual blade tracking, an attempt was made to use in-flight tracking to remove (or attenuate) a remaining imbalance of the rotor which was not completely eliminated during the previous mass balancing procedure. From the blade tracking measurements conducted earlier the influence on 1/rev in-plane forces (sine and cosine of  $F_x$  and  $F_y$ ) of each blade were known and combined into an imbalance vector plot (see Figure 15). For all four blades a linear behavior was found – a blade pitch offset of  $\pm 0.5^\circ$  yields a 1/rev force change of  $\pm 75$  N and a positive offset of one blade has the same influence as a negative offset of the opposite blade. Together with the reference value a rough estimation was made to come to zero in-plane loads. Using offsets of  $+0.35^\circ$  for blade 4 (red) and  $+0.4^\circ$  for blade 3 (blue) the 1/rev in-plane forces could be reduced from 80 N to 12 N (decrease of 85%). On the other hand the in-plane moments are influenced by blade tracking as well because of the change in rotary force. In this single test the pitching moment was increased from 47 Nm to 76 Nm (+60%).

In reality a mixture of tracking for zero in-plane forces and tracking for low mast bending moments is probably the most reasonable solution, depending on which kind of vibration is considered more severe or more harmful for crew and equipment. This test proved the general suitability of the META-system for in-flight tracking and marks an important step towards the adaptive in-flight

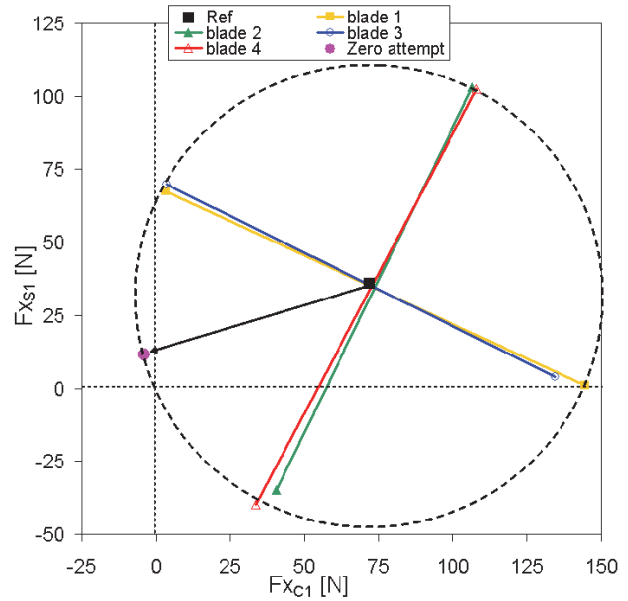


Figure 15 - Imbalance plot with near optimal tracking solution for zero in-plane forces

tracking controller which is currently being developed for use in future wind tunnel tests (see also 6.2).

### 5.4. Higher Harmonic Control 2-6/rev

The HHC tests conducted with the META-system consisted of single-frequency phase sweeps (in  $30^\circ$  and  $60^\circ$  steps) at different control amplitudes up to  $1.5^\circ$  pitch. All scheduled tests were conducted successfully although in some cases the desired blade pitch amplitudes were not reached due to load restraints of the actuator base plates and the rotor blades.

The correlations between commanded and measured pitch amplitude were found to be nearly linear for all controlled frequencies, an examples for 2/rev HHC is shown in Figure 16.

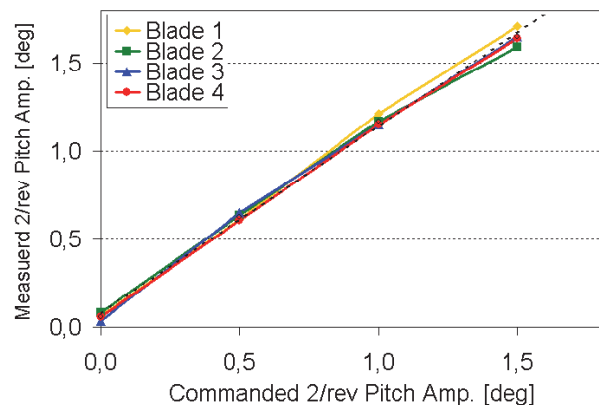


Figure 16 - 2/rev commanded vs. measured pitch amplitude

However, the respective gradients of those linear correlations increased significantly with the controlled frequency. The reason for this behavior is that free play (for example within the ball bearings of the swashplates) and lack of stiffness in the control path (between the

baseplate actuator mount and the pitch links) as well as inertia forces pose a significantly bigger issue at higher frequencies. Further analysis showed that the increase of the measured blade pitch angles (up to 150% increase) is far more pronounced than that of the corresponding actuator strokes (max. 25% increase), see Figure 17.

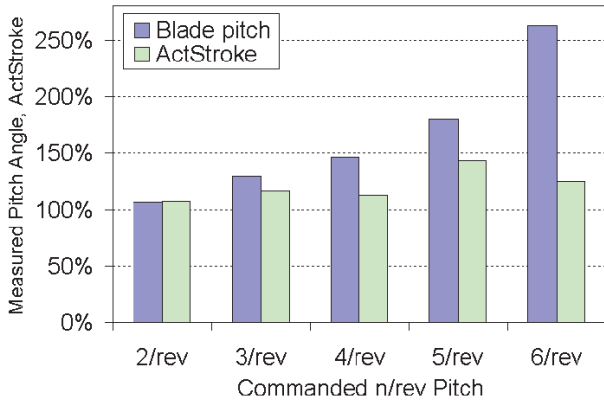


Figure 17 - Pitch and actuator stroke gradients vs. control frequency

This leads to the conclusion that the issues mentioned above mainly apply to the mechanical system above and below the actuators (baseplates, swashplates, pitch links, etc.) and less to the actuators themselves.

During all tests the actuator loads were measured via strain gauges located underneath the baseplates of the actuators (hence referred to as "actuator forces"). The dependencies of the actuator-force / HHC-amplitude gradients (in Newton per deg) on the HHC frequency are depicted in Figure 18 for both the inner and the outer swashplate.

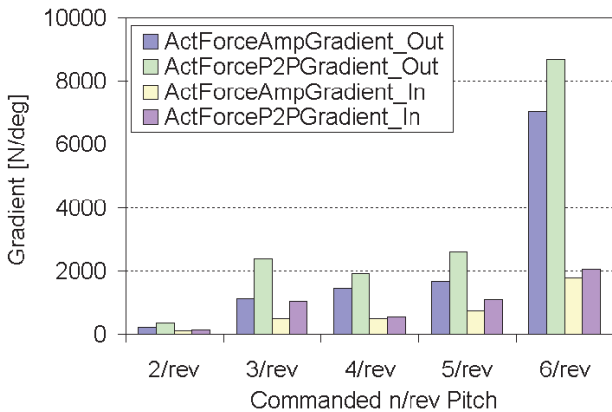


Figure 18 - Actuator force gradients of outer and inner swashplate vs. control frequency

Since 3, 4 and 5/rev HHC are all achieved with 4/rev actuator movements in the non-rotating frame (with control signals only differing in phase), the force gradients for those frequencies are in the same order of magnitude. In the 6/rev case the actuators move the swashplates collectively with a frequency of 6/rev (105 Hz), resulting in considerably higher loads and force gradients. When comparing the general levels of actuator-force gradients for both swashplates, it becomes evident from the data

shown in Figure 18 that the higher mass of the outer swashplate (compared to the inner swashplate) results in higher actuator forces due to increased inertia. The aforementioned problem of free play within the mechanical system is apparent as well. While ideally the force gradients for amplitude and half-peak-to-peak (p2p/2) values should be equal (for each swashplate), differences in excess of 1000N/° were observed. Contrary to the amplitude of the actuator force, which is the result of an FFT and thus only covers the harmonic portion of the alternating load at n/rev frequencies, the p2p/2-value also accounts for load peaks such as shown in Figure 19 for a 3/rev test (actuator frequency 4/rev) which are typical indicators of mechanical free play.

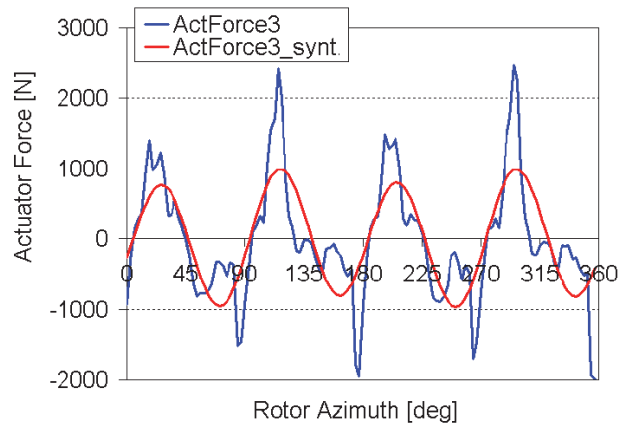


Figure 19 - 4/rev amplitude and half peak-to-peak value of actuator force

Since the limit for dynamic loads on the actuator baseplates is 2000 N, the high p2p/2-loads effectively limited the amplitude for 2, 3, and 4/rev HHC. For the same reason the 6/rev HHC tests, which show a very steep increase of the force gradient (Figure 18) had to be aborted at a control amplitude of only 0.07°. Another limiting factor during the HHC-tests was the torsional moment of the rotor blades.

In addition to the pitch amplitudes and forces, the measured phase angles for all blades measured during the phase sweep for each HHC frequency were analyzed. The phase error between the commanded HHC control signals  $\Theta_{n,CMD}$  and the measured pitch signals of the blades  $\Theta_{n,1-4}$  (normalized to rotor azimuth) was found to be within acceptable limits, although increasing significantly with the control frequency (see Figure 20)

As before with the measured pitch amplitudes, this can be explained by the mechanical properties and mass of the dynamic system, which play a bigger role at higher frequencies and cause a change in dynamic response. While for all frequencies the phase errors for blades 1, 3 and 4 are in agreement, blade 2 exhibits major differences up to about 5°. This can most likely be attributed to free play in the corresponding mechanic components (pitch link, bearings etc.) leading to a distorted pitch sensor signal and thus altering the harmonic analysis of this signal. Further investigations of recordings from the pitch angle sensor of blade 2 also showed a static offset and other discrepancies when compared to the values from blades 1, 3 and 4, justifying the assumption that the blade pitch sensor itself is faulty and needs to be replaced.

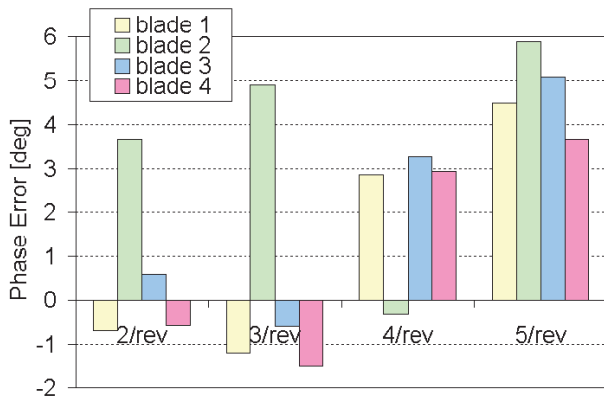


Figure 20 - Phase Errors for all blades and control frequencies

### 5.5. Tip Path Plane-Splitting

The main goal of tip path plane splitting (TPP-splitting) is an increase in miss-distance between the rotor blades' tips and the blade-tip-vortices moving through the rotor disc in order to reduce blade-vortex-interaction (BVI) noise. The concept itself has been described in [23]. While the effect on BVI-noise can only be evaluated in flight tests or a wind tunnel [25], the tests conducted in the DLR's preparation hall were able to prove the general capability of the META-system to achieve this kind of individual blade control. Three different modes were tested, collective, cyclic (1/rev) and 2/rev TPP-splitting.

#### 5.5.1. Collective and Cyclic TPP-Splitting

The first mode, collective TPP splitting is comparatively simple, a differential steady offset of the two swashplates relative to the reference collective. The rotor disk is then effectively split up into two rotor disks with two blades each. The commanded "amplitude" for this mode describes the difference in collective pitch between the rotor blades of the different swashplates and ranged from 0° to 2.5°. As can be seen in Figure 21, collective TPP control was very accurate, resulting in blade pitch angles of exactly ±0.5°, ±1.0° and ±1.25° for the two rotor blades of each swashplate. Since in this special case the collective TPP-splitting is done symmetrically and no cyclic control is applied (as would be the case under normal operating conditions) this mode is entirely free of reaction – no changes in rotor thrust, moments or in-plane hub-forces were measured.

In the cyclic or 1/rev case, first both swashplates were positioned synchronously for a longitudinal cyclic pitch of up to 0.75°. To achieve TPP-splitting, the phase of the control signal for the blades of the second (inner) swashplate was shifted by 180°, resulting in two separate tip path planes, symmetrically tilted against each other (see Figure 22). In addition to testing different 1/rev amplitudes, a phase sweep (30° steps) was conducted to move the locations of maximum TPP displacement to different azimuthal positions. As the cyclic control for the two swashplates was differential (+ $\Theta_C$  on the outer swashplate, - $\Theta_C$  on the inner swashplate) the 4-bladed rotor was effectively split into two two-bladed, hingeless rotor systems sharing one rotor hub. In this configuration the coriolis forces caused by the 1/rev flapping of the

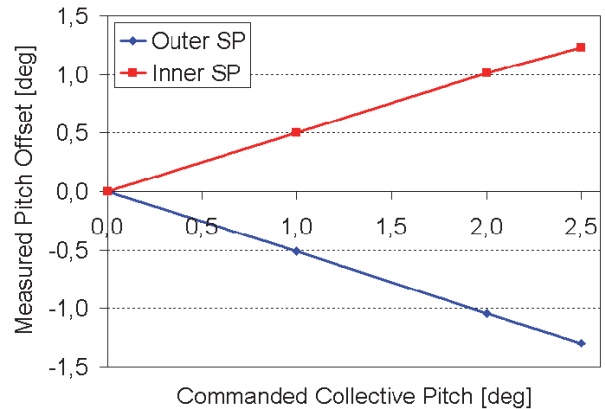


Figure 21 - Measured blade pitches for different collective TPP settings

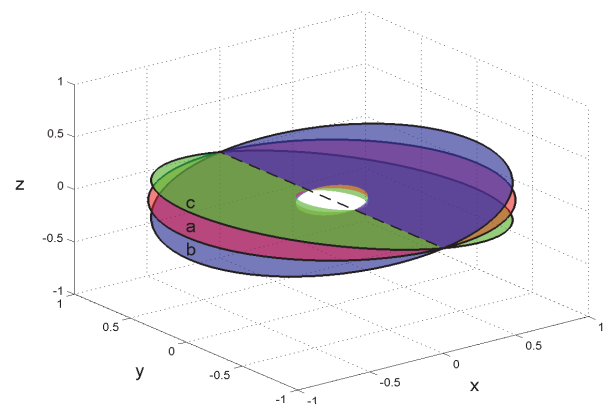


Figure 22 - Schematic of 1/rev TPP splitting: a = reference plane, b and c = splitted planes

blades add up resulting in 2/rev in-plane vibrations proportional to  $\beta \cdot \dot{\beta}$ . Since the longitudinal eigenfrequency of the rotor balance is 32.8 Hz (see 4.1) the system was excited by the 2/rev (approx. 35 Hz) vibrations from the rotor hub leading to significantly higher 2/rev loads than originally expected (see Figure 23).

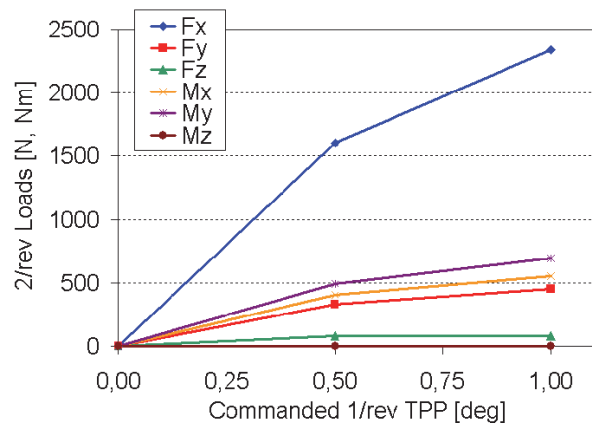


Figure 23 - Increase in 2/rev loads vs. cyclic amplitude during the 1/rev TPP-splitting tests

As a result the x-force transducer exceeded its measurement range and the maximum control amplitude for these tests had to be limited to  $0.75^\circ$  (as opposed to  $1.00^\circ$  originally planned). In order to allow for comparability to the data from the 2/rev TPP splitting tests planned for 50% nominal rotor thrust, the 1/rev TPP-splitting tests were repeated under this thrust condition, yielding similar results.

While the detrimental effect on the in-plane loads was expected, the tests and measurements proved that the 2/rev vibrations and loads may be too high to make 1/rev TPP-splitting feasible as an option to reduce BVI-noise levels. As a consequence, wind-tunnel tests of 1/rev TPP-splitting during the FTK-META will be carried out with reduced control amplitudes.

### 5.5.2. 2/rev TPP-Splitting

The last of the TPP-splitting modes tested was 2/rev TPP splitting at 50% nominal rotor thrust. This was (just as the 1/rev mode) achieved via a  $180^\circ$  phase shift between the control signals for the two sets of blades and caused a 2/rev collective blade flapping for the 4-bladed model rotor. As a result two individual, warped TPPs are generated by 2 blades each (schematic see Figure 24)

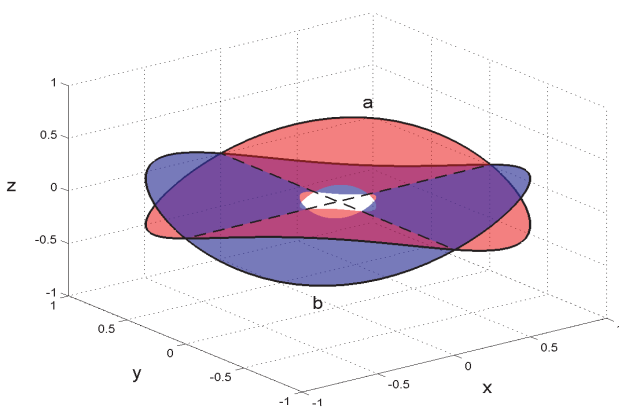


Figure 24 - Schematic of 2/rev TPP-splitting on a 4-bladed rotor

Again, full phase sweeps in  $30^\circ$  steps were conducted for different control amplitudes. In contrast to the 1/rev TPP-splitting, this mode is free of dynamic hub moments; however, due to the  $180^\circ$  phase shift the 2/rev pitch variations of the 4 blades are in phase resulting in relatively large 2/rev thrust oscillations, measured as 2/rev amplitude of the z-force on the rotor balance (see Figure 25)

## 5.6. Difficulties Encountered

Just as in the preliminary tests without blades, during the main tests with blades two noteworthy problems appeared, which made further revisions of the system necessary.

### 5.6.1. De-Coupling of Valve and Actuator

During 4 & 5/rev frequency tests, at amplitudes where the measured loads in the baseplates of the actuators approached their load limits, the above discussed resonance (see 4.4) appeared again. With installed blades

the dynamic response of the dynamic system obviously changed in such a manner that reducing the system pressure was no longer sufficient to prevent those events.

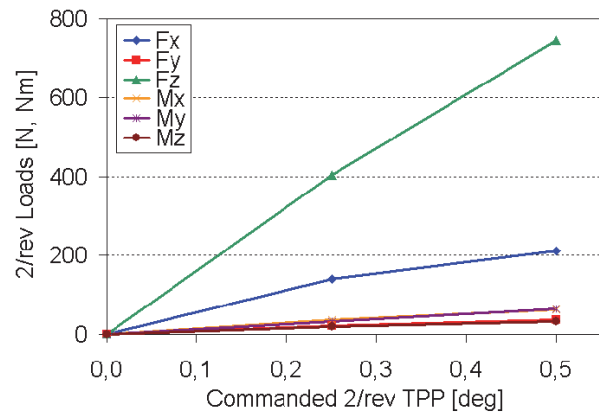


Figure 25 - Increase in 2/rev z-force amplitude vs. 2/rev amplitude (splitTED TPPs)

An analysis of the time response of the actuator strokes showed that in these cases actuator 1 (outer swashplate at very back position) started oscillating first, exciting all other actuators and thus leading to a degradation of the overall system behavior.

The solution to this problem was based on the idea of changing the dynamic characteristic of actuator 1 without losing its control accuracy. The valve was mechanically de-coupled from actuator 1 using short hoses between the actuator and the valve. Additionally, the valve was tilted  $90^\circ$  to prevent interactions of vertical accelerations and the inner valve piston. Due to the increased oil volume in actuator 1 its frequency response changed (additional damping) requiring some parameter changes in the feed forward controller. With this, the problem was finally solved.

### 5.6.2. Implementation of Flushing Sequence

After several test sequences non-predictable events occurred from time to time, causing single actuators to execute spontaneous movements deviating from the commanded stroke. Even though an oil filtering system is used, it is assumed that these movements are related to impurities and particulate matter momentarily blocking the inner piston of the valves or just changing their inner friction properties. Since these events generally occur during steady inputs, where (apart from leak oil) the flow-rate through the valve is zero, a simple flushing sequence was implemented to wash out all possible impurities prior to rotating. During this flushing sequence the actuators perform a collective harmonic motion at 1 Hz with 3 mm amplitude.

## 6. CONCLUSIONS AND OUTLOOK

### 6.1. Hover Tests Results

The main goal of the conducted hover tests was to demonstrate the functionality of the multiple swashplate system for HHC and IBC applications in hover condition. Although some of the test points could only be completed using a smaller control amplitude than planned (see 5.1), all previously scheduled control modes – single frequency

HHC, in-flight blade tracking and several modes of TPP splitting were successfully tested and produced valuable results. The data gathered will be used to further improve and modify the META-system itself as well as the control hard- and software and is the foundation of the preparation for future wind tunnel tests. Without any major incidents or failures and with all planned tests finished within the scheduled time frame the tests of the META system are deemed a success.

## 6.2. Remaining Activities for 2012 and 2013

In 2012 the tested META system will be disassembled and each component will be inspected separately. As described in the test section some components were loaded close to their load limits. It is likely, that in a wind tunnel campaign the static loads of the baseline cases are even higher than in the rotor hall of DLR and the operative range could be even more limited. To counteract this, the respective components will be revised prior to the wind tunnel entry. As an example the stiffness of the rotor balance could be increased to shift the longitudinal eigenfrequency away from the 2/rev frequency and thus to prevent excitation of the rotor balance system by 2/rev hub loads (see 5.5.1).

To test the META in the wind tunnel, the model needs to be covered. So, for the planned tests an existing aeroacoustic fuselage will be adapted to house the modified test rig.

Due to the high loads measured at the baseplates of the actuators mainly due to inertia forces of the swashplates, it is also currently discussed to modify some parts of the META to reduce its weight.

In preparation of the planned wind tunnel test a new set of modern model rotor blades will be constructed and built together with Eurocopter Germany in 2012 and 2013 to enable a comparison to the measurements gathered with the old set of rectangular Bo105 model rotor blades. Since the blades tested on the META system showed much higher torsional loads than expected, a set of refurbished and instrumented Bo105 model rotor blades from the HART II campaign will be used in the wind tunnel test. Those blades previously showed significantly lower torsional loads under similar test conditions and also allow for accurate comparison of the results from the wind tunnel tests of the META-system and the HART II test.

Additionally, in 2012 and 2013 a new controller will be developed and tested (in simulation) using the single-blade tracking task mode for vibration reduction. The goal is to test this controller in the wind tunnel campaign.

Finally, the results of the completed META campaign in the test hall of DLR will find their way to enhance the DLR's rotor simulation code S4.

## 6.3. Future Plans for META

The preliminary META tests were part of the national aeronautical research program "Vollaktive Rotorsteuerung" (Fully active rotor control, VAR) in co-operation with Eurocopter Germany funded by the German Ministry of Economics (BMW), ending in September 2012. These successful tests serve as preparation to the follow-up program "Fortschrittliche Taumelscheibenkonzepte" (Advanced swashplate concepts, FTK) again in co-operation with Eurocopter

Germany, also funded by the German Ministry of Economics, started in 2012 and ending in 2015. Within this project DLR will bring the META system into the large low speed wind tunnel of the DNW to test all individual control issues developed in VAR-META. These tests also will support Eurocopter's development of their 2/rev double-swashplate system through extensive 2/rev tests. Currently the wind tunnel entry is planned for the first half-year of 2014.

## REFERENCES

- [1] W. Stewart, "Second Harmonic Control on the Helicopter Rotor," *Journal of the Royal Aeronautical Society*, vol. 2997, no. 2472, pp. 1-15, 1952.
- [2] P. R. Payne, "Higher Harmonic Control: The Possibilities of Third and Higher Harmonic Feathering for Delaying the Stall Limit in Helicopters," *Aircraft Engineering*, vol. 30, no. 8, pp. 222-226, 1958.
- [3] P. J. Arcidiacono, "Theoretical Performance of Helicopters Having Second and Higher Harmonic Feathering Control," *Journal of the American Helicopter Society*, vol. 6, no. 2, pp. 8-19, 1961.
- [4] R. K. Wernicke and J. M. Drees, "Second Harmonic Control," in *Proceedings of the 19th Annual National Forum of the American Helicopter Society*, Washington D.C., USA, 1963, pp. 1-7.
- [5] E. R. Wood, R. W. Powers, J. H. Cline, and C. E. Hammond, "On Developing and Flight Testing a Higher Harmonic Control System," *Journal of the American Helicopter Society*, vol. 30, no. 1, pp. 3-20, 1985.
- [6] W. R. Splettstoesser, K.-J. Schultz, R. Kube, T. F. Brooks, E. R. Booth, G. Niesl, and O. Streby, "A Higher Harmonic Control Test in the DNW to Reduce Impulsive BVI Noise," *Journal of the American Helicopter Society*, vol. 39, no. 4, pp. 3-13, 1994.
- [7] T. R. Norman, C. Theodore, P. Shinod, D. Fürst, U. T. P. Arnold, S. Makinen, P. Lorber, and J. O'Neill, "Full-Scale Wind Tunnel Test of a UH-60 Individual Blade Control System for Performance Improvement and Vibration, Loads and Noise Control," in *Proceedings of the 65th Annual Forum of the American Helicopter Society*, Fort Worth, TX, USA, 2009.
- [8] P. Richter and A. Blaas, "Full Scale Wind Tunnel Investigation of an Individual Blade Control (IBC) System for the BO 105 Hingeless Rotor," in *Proceedings of the 19th European Rotorcraft Forum*, Washington D.C., USA, 1980.
- [9] S. A. Jacklin, S. Swanson, A. Blaas, P. Richter, D. Teves, G. Niesl, R. Kube, B. Gmelin, and D. L.

- Key, "Investigation of a Helicopter Individual Blade Control (IBC) System in Two Full-Scale Wind Tunnel Tests," 2003.
- [10] N. D. Ham, "A Simple System for Helicopter Individual-Blade-Control and its Application to Gust Alleviation," in *Proceedings of the 6th European Rotorcraft Forum*, Bristol, UK, 1980.
- [11] N. D. Ham, B. L. Behal, and R. M. McKillip, "Helicopter Lag Damping Augmentation Through Individual-Blade-Control," *VERTICA - The International Journal of Rotorcraft and Powered Lift Aircraft*, vol. 7, no. 4, pp. 361-371, 1983.
- [12] T. R. Quackenbush, "Testing and Evaluation of a Stall-Flutter-Suppression System for Helicopter Rotors using Individual-Blade-Control," *Journal of the American Helicopter Society*, vol. 29, no. 2, pp. 38-44, 1994.
- [13] G. Reichert, "Helicopter Vibration Control - A Survey," *VERTICA - The International Journal of Rotorcraft and Powered Lift Aircraft*, vol. 5, no. 1, pp. 1-20, 1981.
- [14] A. C. Veca, "Vibration Effects on Helicopter Reliability and Maintainability," U.S. Army Air Mobility Research and Development Laboratory, Fort Eustis, VA, 1973.
- [15] W. R. Spletstoesser, B. G. van der Wall, B. Junker, K.-J. Schultz, P. Beaumier, Y. Delrieux, P. Leconte, and P. Crozier, "The ERATO Programme: Wind Tunnel Results and Proof of Design for an Aeroacoustically Optimized Rotor," in *Proceedings of the 25th European Rotorcraft Forum*, Rome, Italy, 1999.
- [16] C. Kessler, "Active Rotor Control for Helicopters - Motivation and Survey on Higher Harmonic Control," in *Proceedings of the 36th European Rotorcraft Forum*, Paris, France, 2010.
- [17] C. Kessler, "Active Rotor Control for Helicopters - Individual Blade Control and Swashplateless Rotor Designs," in *Proceedings of the 36th European Rotorcraft Forum*, Bristol, UK, 2010.
- [18] D. Roth, B. Enenkl, and O. Dieterich, "Active Rotor Control by Flaps for Vibration Reduction - Full Scale Demonstrator and First Flight Test Results," in *Proceedings of the 28th European Rotorcraft Forum*, Bristol, 2006.
- [19] F. K. Straub, V. R. Anand, T. S. Birchette, and B. H. Lau, "Wind Tunnel Tests of the SMART Active Flap Rotor," in *Proceedings of the 65th Annual Forum of the American Helicopter Society*, Fort Worth, TX, USA, 2009.
- [20] J. Riemenschneider, S. Opitz, P. Wierach, H. des Rochettes, and L. Buchanek, "Structural Design and Testing of Active Twist Blades - A Comparison," in *Proceedings of the 35th European Rotorcraft Forum*, Hamburg, Germany, 2009.
- [21] B. G. van der Wall and R. Bartels, "Patent für eine Hubschrauber-Rotorsteuereinrichtung," Patent-Nr.: 102006030089, Deutsches Patent- und Markenamt, Germany, 2008.
- [22] R. Bartels, P. Küfmann, and C. Kessler, "Novel Concept for Realizing Individual Blade Control (IBC) for Helicopters," in *Proceedings of the 36th European Rotorcraft Forum*, Paris, France, 2010.
- [23] P. Küfmann, R. Bartels, C. Kessler, and B. G. van der Wall, "On the Design and Development of a Multiple-Swashplate Control System for the Realization of Individual Blade Control for Helicopters," in *Proceedings of the 67th Annual Forum of the American Helicopter Society*, Virginia Beach, VA, USA, 2011.
- [24] B. Geelhaar, K. Alvermann, and F. Dzaak, "A Rotor Acoustic Data Acquisition System Based On Transputers and Delta-Sigma Converters," in *Proceedings of the European Test and Telemetry Conference*, Toulouse, France, 1991.
- [25] B. G. van der Wall, B. Junker, C. L. Burley, T. F. Brooks, Y. H. Yu, C. Tung, M. Raffel, H. Richard, W. Wagner, E. Mercker, K. Pengel, H. Holthusen, P. Beaumier, and Y. Delrieux, "The HART II Test in the LLF of the DNW - a major step towards rotor wake understanding," in *Proceedings of the 28th European Rotorcraft Forum*, Bristol, UK, 2002.